Photochemical & Photobiological Sciences

Accepted Manuscript

This is an *Accepted Manuscript*, which has been through the Royal Society of Chemistry peer review process and has been accepted for publication.

Accepted Manuscripts are published online shortly after acceptance, before technical editing, formatting and proof reading. Using this free service, authors can make their results available to the community, in citable form, before we publish the edited article. We will replace this *Accepted Manuscript* with the edited and formatted *Advance Article* as soon as it is available.

You can find more information about *Accepted Manuscripts* in the Information for Authors.

Please note that technical editing may introduce minor changes to the text and/or graphics, which may alter content. The journal's standard Terms & Conditions and the Ethical guidelines still apply. In no event shall the Royal Society of Chemistry be held responsible for any errors or omissions in this *Accepted Manuscript* or any consequences arising from the use of any information it contains.

ROYAL SOCIETY OF CHEMISTRY

www.rsc.org/pps

Kinetic Analysis of Nitroxide Radical Formation Under Oxygenated Photolysis: Toward Quantitative Singlet Oxygen Topology

David F. Zigler, Eva Chuheng Ding, Lauren E. Jarocha, Renat R. Khatmullin, Vanessa DiPasquale, R. Brendan Sykes, Valery F. Tarasov, Malcolm D. E. Forbes*

Department of Chemistry
University of North Carolina at Chapel Hill
Chapel Hill, NC 27599, USA
*mdef@unc.edu

Abstract: Reaction kinetics for two sterically hindered secondary amines with singlet oxygen have been studied in detail. A water soluble porphyrin sensitizer, 5,10,15,20-tetrakis-(4-sulfunatophenyl)-21,23H-porphyrin (TPPS), was irradiated in oxygenated aqueous solutions containing either 2,2,6,6-tetramethylpiperidin-4-one (TMPD) or 4-[N,N,N-trimethyl-ammonium]-2,2,6,6-tetramethylpiperidinyl chloride (N-TMPCl). The resulting sensitization reaction produced singlet oxygen in high yield, ultimately leading to the formation of the corresponding nitroxide free radicals (R_2NO) which were detected using steady-state electron paramagnetic resonance (EPR) spectroscopy. Careful actinometry and EPR calibration curves, coupled with a detailed kinetic analysis, led to a simple and compact expression relating the nitroxide quantum yield Φ_{R2NO} (from the doubly-integrated EPR signal intensity) to the initial amine concentration $[R_2NH]_i$. With all other parameters held constant, a plot of Φ_{R2NO} vs. $[R_2NH]_i$ gave a straight line with a slope proportional to the rate constant for nitroxide formation, k_{R2NO}. This establishment of a rigorous quantitative relationship between the EPR signal and the rate constant provides a mechanism for quantifying singlet oxygen production as a function of its topology in heterogeneous media. Implications for *in vivo* assessment of singlet oxygen topology are briefly discussed.

Introduction

Considerable interest in understanding oxidative stress mechanisms within cells has driven the desire to detect reactive oxygen species (ROS) with high spatial resolution.[1] With the rise of the use of photosensitizers and light in the treatment of cancer (photodynamic therapy, PDT),[2,3] significant interest has been focused on the distribution and production of molecular oxygen in its lowest singlet excited states (ES) ($^1O_2$ = total population of ES, $^1\Delta g + {}^1\Sigma_g$).[4-7] While several methods exist, none can directly and quantitatively measure the local population of ROS and identify specific regions of action on the nanometer scale. The best approach to determine singlet oxygen topology will use a diverse array of techniques to construct an image of oxidative damage within a cell or other heterogeneous structure.

Electron paramagnetic resonance spectroscopy (EPR) can be used to detect radical products resulting from reactions with ROS in biological media. The technique has high sensitivity (> 10^8 spins per sample) and selectivity for some radical species.[8] Observation of the photosensitized oxidation of sterically hindered secondary amines to their EPR–active nitroxide analogs is interpreted as confirmation of the presence of $^1O_2$ (shown in Scheme 1, for example, is the water-soluble photosensitizer 5,10,15,20-tetrakis-(4-sulfunatophenyl)-21,23H-porphyrin (TPPS)).

Scheme 1

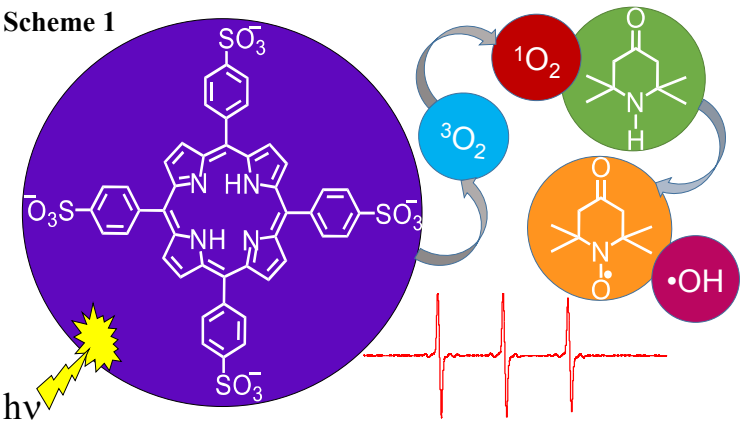

Recent studies of this reaction include the transformation of 2,2,6,6-tetramethylpiperidin-4-one (TMPD) and 4-[N,N,N-trimethyl-ammonium]-2,2,6,6-tetramethylpiperidinyl chloride (N-TMPCl) to their corresponding nitroxides (TEMPOne, N-TMPO).[9]

Chart 1

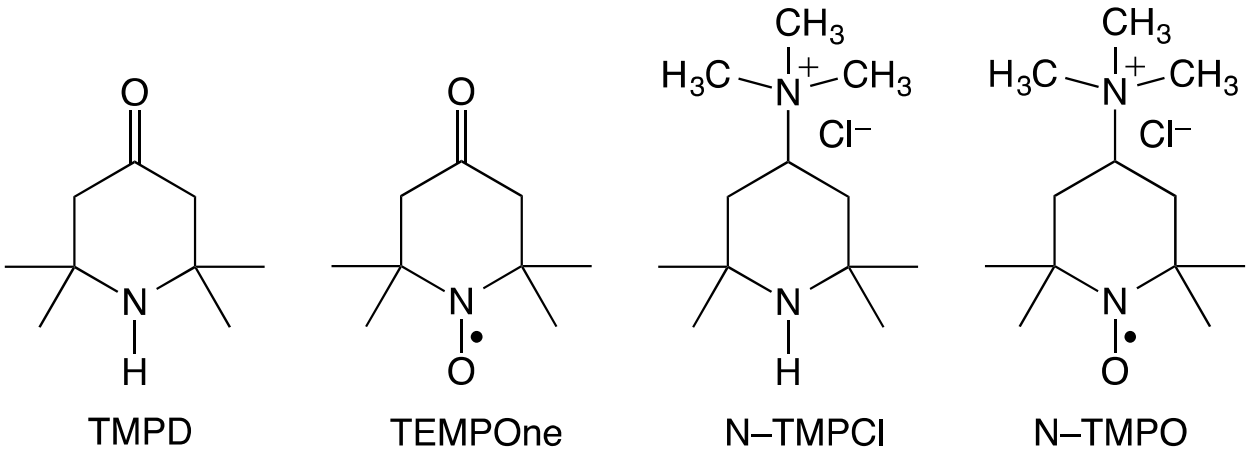

The reaction in Scheme 1 is extensively used for qualitative confirmation of the presence of $^1O_2$,[10-23] however few quantitative kinetic studies have been performed. The widespread use of this reaction for confirmation of $^1O_2$ is surprising given the controversy over the mechanism of nitroxide formation and the associated reaction kinetics. For example, several kinetic studies have yielded contradictory rate constants (varying over four orders of magnitude) for the formation of nitroxide radicals from compounds like TMPD.[24-32] Additionally, the selectivity of hindered secondary amines for $^1O_2$ has been disputed.[31-37] Clearly, the current status of the field warrants a detailed examination of the nitroxide formation reaction under conditions analogous to those used in *in vitro* and *in vivo* PDT experiments. Herewith, we report a reexamination of the kinetics of nitroxide formation from TMPD and N-TMPCl under physiologically relevant conditions. The water-soluble photosensitizer 5,10,15,20-tetrakis-(4-sulfunatophenyl)-21,23H-

porphyrin (TPPS) was used under flowing oxygen, in buffered aqueous solutions, with 395(±5) nm illumination. After photolysis and purging with nitrogen, steady state EPR was used to measure the concentration of nitroxide formed. Transient absorption spectroscopy (on the ns to ms timescales) was used to understand what influence competing reactions had on the observed kinetics.

Background

There are many events leading to the production and decay of $^1O_2$ after the excitation of a sensitizer such as TPPS, and there are several important side reactions of $^1O_2$ with amine starting materials or nitroxide products that should be considered in regard to $^1O_2$ reaction kinetics. These processes are summarized in Scheme 2, which is divided into additional sub-sections for clarity.

Scheme 2

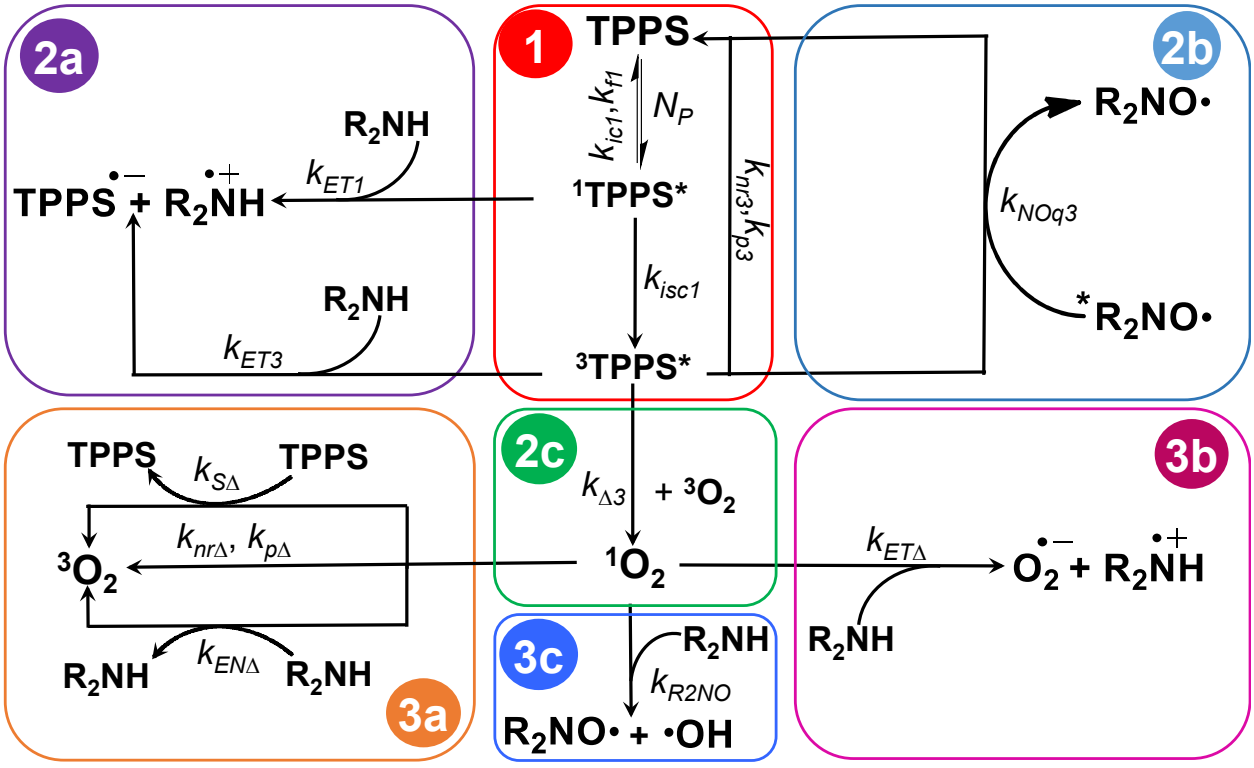

Scheme 2–1: Native Relaxation

In dilute, buffered (pH = 8) aqueous solution TPPS exists in monomeric form, free from aggregation.[38] Excitation of TPPS occurs following absorption of light from the ultraviolet and visible regions of the spectrum. In the absence of oxygen or other quenchers, the initially populated singlet state, ^{1}TPPS* ($\Delta E_{(1*\text{-}GS)}$ = 1.92 eV), relaxes to the ground state (GS) with a lifetime τ_1 = 10 ns. Relaxation may occur by fluorescence (k_{f1}), internal conversion (k_{ic1}) or intersystem crossing (k_{isc1}).[39-42] The first two processes result in repopulation of the ground state, while intersystem crossing gives the lower energy excited triplet state, ^{3}TPPS* ($\Delta E_{(3*\text{-}GS)}$ = 1.44 eV). The ^{3}TPPS* state also relaxes by non-radiative (k_{nr3}) and radiative (k_{p3}) pathways, though on a much longer timescale (τ_3 = 510 μs).[39-41]

Scheme 2–2a: *Excited State Porphyrin Quenching by Amines*

Hindered amine light stabilizers (HALS)[43] like 2,2,6,6-tetramethyl-piperidin-4-one, TMPD are used to decrease damage caused by direct (type I) and singlet oxygen mediated (type II) photo-oxidation of polymers. If the amines examined in this paper react with the excited photosensitizer, we could see inflated or deflated yields for the production of nitroxide due formation of radical precursors or interference in singlet oxygen production. The standard oxidation potential of TMPD has not been measured. Instead, peak potentials of an irreversible oxidation are listed as 1.18 V vs. SCE[44] and 1.14 V vs. Ag/Ag$^+$ in wet acetonitrile.[45] Electron transfer quenching of the ^{1}TPPS* and ^{3}TPPS* by TMPD or similar HALS (k_{ET1}, k_{ET3}) is thermodynamically unfavorable for amines where the first amine oxidation occurs at potentials positive of <0.86 or <0.38 V vs NHE[40,46,47] for ^{1}TPPS* or ^{3}TPPS* state, respectively.[48] Photo-oxidation of various tertiary amines or aniline by the electron deficient

tetrakis(perfluorphenyl)porphyrin followed Marcus theory in dichloromethane, but no quenching was observed of porphyrins with more electron rich phenyl substituents.[49]

Scheme 2-2b: Energy Transfer Quenching to Nitroxide

Nitroxides like TEMPOne are efficient quenchers of excited triplet states, often with diffusion limited second-order rates constants ($k_{NOq3} \sim 10^{10}$ s^{-1}).[50.51] Build-up of nitroxide in the solution therefore provides an additional quenching pathway for the TPPS triplet. Due to the very low concentrations of nitroxide produced during our photolysis experiments, it unlikely that this pathway has much impact on our observed kinetics.

Scheme 2-2c: Energy Transfer Quenching to Oxygen (Singlet Oxygen Generation)

Molecular oxygen, $^3O_2$, efficiently quenches the triplet state of TPPS, shortening the excited state lifetime to 1.9 μs in air.[52,53] Single electron reduction of oxygen ($^3O_2 \rightarrow O_2^{-\cdot}$, $E° = -0.33$ V vs. NHE) by both ^{1}TPPS* and ^{3}TPPS* is thermodynamically favored and may also contribute to the observed photobleaching of TPPS in aerated buffer (quantum yield for photobleaching $\Phi_{PB} = 9.8 \times 10^{-6}$).[54] Energy transfer dominates the quenching dynamics, giving the excited singlet state of oxygen, $^1O_2$ ($k_{\Delta 3}$), with high quantum yield ($\Phi_\Delta = 0.6$ in O_2-saturated buffer).[55]

Schemes 2–3a,2–3b: Singlet Oxygen Relaxation, Chemical and Physical Quenching

Singlet oxygen relaxes to the ground state rapidly by vibrational coupling to the solvent ($k_{nr\Delta}$) or by phosphorescence ($k_{p\Delta}$) to form triplet oxygen. Due to the high frequency O-H stretch of water, the lifetime of $^1O_2$ (τ_Δ) is 3.1 μs.[56] Ground state TPPS is non-innocent, rapidly quenching $^1O_2$ by a physical mechanism ($k_{S\Delta}$). In D_2O, $k_{S\Delta} = 2 \times 10^9$ $M^{-1}s^{-1}$ and is thought to be the same in water

(Scheme 2–3a).[55] There is no evidence for reduction of $^1O_2$ to superoxide, $O_2^{-\cdot}$ by ground state TPPS. The reaction of $^1O_2$ with amines is complicated.[43,57-59] There is evidence that $^1O_2$ forms a charge transfer complex with amines,[60] and that this complex can decay to give either ground state starting materials ($k_{EN\Delta}$, Scheme 2–3a) or some redox products ($k_{ET\Delta}$, Scheme 2–3b). The estimated 1 electron reduction potential of $^1O_2$ ($E^{*/-} \approx 0.6$ V vs NHE) is likely too negative to oxidize TMPD to the TMPD radical or radical cation by electron transfer.[61]

Scheme 2–3c: *Formation of Nitroxide*

Reaction of $^1O_2$ with TMPD produces the corresponding nitroxide (k_{R2NO}), where k_{R2NO} is some proportion of the total amine quenching constant ($k_{q\Delta}$) and may not reflect the total chemical quenching pathway. This allows us to express the quantum yield for nitroxide formation (Φ_{R2NO}) as eq 1:

$$\Phi_{R2NO} = \Phi_{\Delta} \cdot \frac{k_{R2NO}[R_2NH]_i}{k_{p\Delta} + k_{nr\Delta} + k_{q\Delta}[R_2NH]_i + k_{S\Delta}[TPPS]} \quad (1)$$

where Φ_{R2NO} is measured as the number of nitroxide molecules produced per absorbed photon. Two predictions result from this kinetics expression. First, Φ_{R2NO} should be linear with respect to the initial concentration of TMPD at concentrations where the total quenching of $^1O_2$ by TMPD is much less than the sum of all other relaxation pathways. As the condition $k_{EN\Delta}$ $[TMPD]_i >> 1/\tau_{\Delta}$ is satisfied, the slope approaches $k_{R2NO}/ k_{EN\Delta}$. If $k_{ET\Delta}$ is truly rate limiting step, then the apparent $k_{R2NO} = k_{EN\Delta}$ and the reaction will be zero order ($= \Phi_{\Delta}$) at high concentrations of TMPD.

Equation 1 provides a quantitative relationship between a set of known ($k_{p\Delta}$, $k_{nr\Delta}$, $k_{q\Delta}$, $k_{S\Delta}$, Φ_{Δ}) and measurable ($[R_2NH]_i$, Φ_{R2NO}) quantities from which a rate constant can be extracted.

Below we present calibration curves showing a linear relationship between nitroxide concentration, [TEMPOL], and integrated EPR signal intensity, quantum yield data as a function of $[R_2NH]_i$ and show how this information can be used, via Eq. 1, to quantitatively evaluate k_{R2NO} for amines of different structure. With careful consideration of all of the processes shown in Scheme 2, coupled with the execution of high precision actinometry measurements in these systems for the first time, our results represent the most accurate determination of this rate constant to date. This is relevant for researchers in the field of photodynamic therapy, where quantification and topology of singlet oxygen production are highly desirable.

Results and Discussion

The water soluble photosensitizer TPPS was chosen because it has well characterized solution behavior and spectroscopic properties,[38-42] a known quantum yield of the formation of the triplet excited state (Φ_T) under our experimental conditions,[53] and also a known quantum yield for the formation of $^1O_2$ (Φ_Δ) in oxygen saturated solution.[55,62] In addition, the maximal absorption of the TPPS Soret band[39] overlaps well with the excitation wavelength (395 nm) giving highly absorbing solutions with low concentrations of photosensitizer ($\varepsilon^{413\ nm} = 3.7 \times 10^5$ $M^{-1}cm^{-1}$). The piperidine derivatives 2,2,6,6-tetramethylpiperidin-4-one, TMPD, and 4-[N,N,N-trimethyl-ammonium]-2,2,6,6-tetramethylpiperidinyl chloride, N-TMPCl, were chosen because they are water soluble and have a significant concentration of the free base at physiological *p*H. A slightly basic solution (*p*H 8.0) was chosen to minimize TPPS aggregation[38] and because protonation of TMPD and/or N-TMPCl inhibits its reaction to form TEMPOne or N-TMPO.[27] The initial concentration of amines $[TMPD]_i$ and $[N\text{-}TMPCl]_i$ was calculated using the measured *p*H of the photolysis solution and the Henderson-Hasselbalch equation.

Nitroxide Formation and Detection. Figure 1 shows representative EPR spectra (unnormalized) obtained after 395 nm CW photolysis of the system in Scheme 1 at different photolysis times. EPR signal due to nitroxide increased linearly with photolysis time. Minor background nitroxide signal, which was present in TMPD and N-TMPCl samples prior to photolysis, was accounted for by subtracting the spectrum of an identical solution kept in the dark.

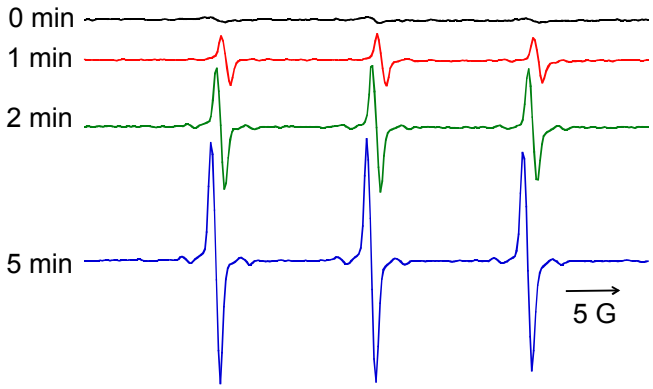

Figure 1. EPR spectra collected during photolysis of 50 mM TMPD in 50 mM aqueous phosphate buffered adjusted to *p*H =8.0 (0 min-black; 1 min-red; 2 min-green; 5 min-blue). [TPPS] was kept constant at 20 mM. EPR samples were prepared by drawing N_2 deaerated solutions into 0.5 mm ID glass capillaries and sealed.

Omission of any of photosensitizer, amine, light or oxygen in the appropriate control reactions gave no measureable photoproduct. EPR experiments ruled out TEMPOne production directly from TMPD oxidation by ^{1}TPPS* or ^{3}TPPS*. Photolysis of TMPD and TPPS under flowing nitrogen gave no EPR signal, nor did oxygen-free photolysis followed by sparging with O_2 in the dark. Photolysis of TPPS under a O_2 atmosphere and adding TMPD afterward also produced no EPR–active compounds. Reactions in which known $^1O_2$ quenchers were added decreased the rate of production of nitroxide, further supporting a $^1O_2$ dependent mechanism.

EPR Calibration Curves. To quantify the nitroxide in solution, samples were deoxygenated afer photolysis and then observed by EPR spectroscopy. Concentration measurements were made by comparing the integrated peak area of the nitroxide signal to a calibration curve plotting

instrument response as a function of known TEMPOL nitroxide concentration (Figure 2). The predominant source of error in the measurement of nitroxide signal was the variation in capillary diameter (±10%), as is evident from the near constant percent deviation within a sample set.

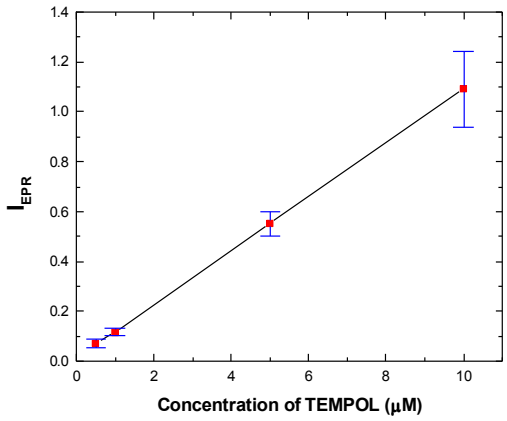

Figure 2. A typical EPR calibration curve measured over the range of TEMPOL concentrations (0.5-10 mM) in 50 mM aqueous sodium phosphate buffer at *p*H = 8.0.

Quantum Yield for Nitroxide Formation. The quantum yield of nitroxide formation (Φ_{R2NO}) was measured for photolysis reactions with different concentrations of TMPD and with different concentrations of TPPS. The Φ_{R2NO} is defined from the experimental observation of the rate of nitroxide formation (dN_{R2NO}/dt) relative to the rate of photons delivered (dN_P/dt). A proportionality constant accounts for the portion of photons absorbed as measured from the electronic absorption spectrum of the photolysis solution. When integrated over all time for steady-state photolysis the Φ_{R2NO} simplifies to $N_{R2NO}/(1-I/I_o)\cdot N_P$, where N_{R2NO} is the number of photogenerated nitroxides measured by EPR and N_P is the total number of photons delivered determined from chemical actinometry.

Although the rate of nitroxide formation varied with LED power, the measured Φ_{R2NO} was insensitive to light flux (4.3×10^{-7} to 4.3×10^{-6} einstein/s) or to photolysis time (Figures 3A and 3B). For photolysis in which [TPPS] > 20 μM, the integrated OD was > 3, giving near unit

absorption of the delivered photons. When keeping the $[TMPD]_i$ constant and correcting for differences in absorbance, the Φ_{R2NO} was independent of [TPPS] in the range of 5 to 45 μM (Figure 3C) indicating no higher order effects due to aggregation of the photosensitizer. Further, we can assume that the $k_{S\Delta}[TPPS]$ is much smaller than the other terms in the denominator of equation 1.

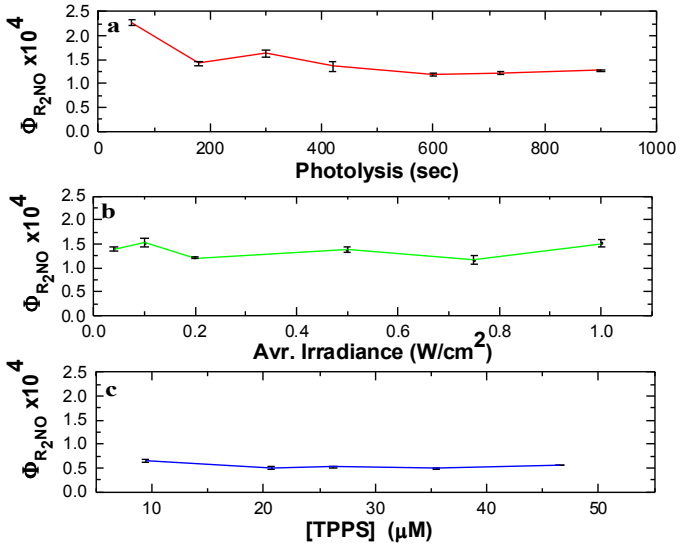

Figure 3. Plot of TEMPOne formation quantum yield as a function of **a**) photolysis time; photolysis time was varied from 60-900 sec. **b**) light power; Light was attenuated by adjusting the LED power supply (4-100% power) with a light flux varying from 4.3 x 10^{-7} to 4.3 x 10^{-6} einstein/s; **c**) photosensitizer TPPS. TPPS concentration was varied from 10-45 μM. The concentration of TMPD·HCl was kept constant at 50 mM (37 mM free base) for **a** and **b**, and 15 mM (9.9 mM free base) in **c**. All solutions were prepared in 50 mM aqueous phosphate buffered adjusted to pH =8.0. Concentration of TPPS in **a** and **b** cases was 20 μM. EPR samples were prepared by drawing N_2 deaerated solutions into 0.5 mm ID glass capillaries and sealed.

Analysis of Nitroxide Formation Kinetics. Nitroxide formation proceeds from a hindered amine in the presence of light, a photosensitizer and oxygen. Careful experiments were performed to quantify, where possible, the important reactions outlined in Scheme 2 that may compete with nitroxide formation. These rates or quantum yields are presented in Table 1, as are relevant literature provided kinetic constants.

Table 1. Selected Rate Constants, Conditions and Definitions

Process		Rate Constant	Conditions	Quantum yield	Ref[a]
Singlet Photosensitizer Relaxation: Internal conversion (k_{ic1}), Fluorescence (k_{f1}), Intersystem crossing (k_{isc1})					
Singlet lifetime	τ_1^{-1}	1.0 x 10^8 s^{-1}	Water	--	39
Triplet Photosensitizer Relaxation: Non-radiative decay (k_{nr3}), Phosphorescence (k_{p3})					
	τ_3^{-1}	2.0 x 10^3 s^{-1}	Deoxygenated	--	39-42
Triplet lifetime	τ_3^{-1}	5.3 x 10^5 s^{-1}	Air	--	53
	τ_3^{-1}	2.2 x 10^6 s^{-1}	O_2	--	t.w.
Excited Photosensitizer Quenching					
Electron transfer from amine	k_{ET1}	$<10^7$ $M^{-1}s^{-1}$	Ar or O_2	--	t.w.
Electron transfer from amine	k_{ET3}	$<10^3$ $M^{-1}s^{-1}$	Ar or O_2	--	t.w.
Energy transfer to nitroxide	k_{NOq3}	6 x 10^7 $M^{-1}s^{-1}$	Air	--	t.w.
Energy transfer to O_2 ($^1O_2$ generation)	$k_{\Delta 3}$	5.3 x 10^5 s^{-1} (τ_3^{-1})	Water, O_2	0.60	56,62
Singlet Oxygen Relaxation: Non-radiative decay ($k_{nr\Delta}$), Phosphorescence ($k_{p\Delta}$)					
Singlet lifetime	τ_Δ^{-1}	2.3 x 10^5 s^{-1}	Water		56,60
Singlet Oxygen Quenching					
Energy transfer to porphyrin	$k_{S\Delta}$	2 x 10^9 $M^{-1}s^{-1}$	--	--	55
Energy transfer to amine	$k_{EN\Delta}$	$<10^4$ $M^{-1}s^{-1}$	CF_3CH_2OH	--	60
Electron transfer from amine	$k_{ET\Delta}$	$<10^4$ $M^{-1}s^{-1}$	CF_3CH_2OH	--	60
Energy transfer to nitroxide	$k_{NOq\Delta}$	4.5 x 10^5 $M^{-1}s^{-1}$	Benzene	--	50,51
Nitroxide Formation					
		1.6 x 10^5 $M^{-1}s^{-1}$	EtOH,	--	30
		4 x 10^7 $M^{-1}s^{-1}$	pH 8	--	29
		2.9 x 10^3 $M^{-1}s^{-1}$	EtOH:Benzene	--	25
		--	pH 7	5 x 10^{-4}	26
Nitroxide Formation	k_{R2NO}	--	pH 9	4.1 x 10^{-3}	27
		5.2 x 10^6 $M^{-1}s^{-1}$	DMSO	--	31
		5.0 x 10^{-7} $M^{-1}min^{-1}$	pH 7.4	1 x 10^{-3}	32
		5 x 10^5 $M^{-1}s^{-1}$	Organic solvents	--	37
		1.0 x 10^4 $M^{-1}s^{-1}$	pH 8	--	t.w.

[a] t.w. = this work

Transient absorption spectra show no evidence for ^{1}TPPS* or ^{3}TPPS* reacting directly with the amine (Supporting Information, Figures S1-S4), only rapid quenching of the triplet by O_2. With and without TMPD, the transient spectra have the same features, indicating no new absorbing species result from a reaction between excited TPPS and the amine. Transient decays indicate similar dynamics with or without added TMPD (SI, Figures S5-S10). In deaerated buffer the lifetime of ^{1}TPPS* was 11(±1) ns with and 10.1(±0.5) ns without TMPD, very close to the literature value. The lifetimes were also similar to each other in oxygenated buffer at 11.7(±0.3) ns with and 10.7(±0.2) ns without TMPD, indicating that TMPD likely does not quench the ^{1}TPPS* state and giving an upper estimate of the quenching rate constant $k_{ET1} < 10^7$ $M^{-1}s^{-1}$. The kinetics of ^{3}TPPS* in deaerated buffer were more difficult to interpret because the triplet state is sensitive to even minute concentrations of oxygen, giving lifetimes of 200 to 450 μs, but with no apparent dependence on TMPD. The lifetimes measured under flowing O_2 were much shorter, ~510 ns with or ~450 ns without TMPD. Although the fits to the decays in oxygenated solutions appear to differ between samples with and without TMPD, the data from each overlay one another, indicating that the variation is probably due to fitting the noisy data and not due to added TMPD. Given all these observations, the absolute maximum of k_{ET3} is estimated to be less than 10^3 $M^{-1}s^{-1}$.

Quenching of ^{3}TPPS* by nitroxide was also examined by TA (SI, Figure S11). TEMPOL, a nitroxide closely related to the photoproduct TEMPOne, is a weak quencher of ^{3}TPPS*, showing enhancement of ^{3}TPPS* decay with [TEMPOL] > 10 mM. At 10 mM TEMPOL, the excited state decays at roughly 4 times the unquenched rate in aerated solution, allowing an estimate of $k_{qNO3} = 6 \times 10^7$ $M^{-1}s^{-1}$. Considering that the maximal concentration of

TEMPOne achieved under the photolysis conditions in these experiments is less than 12 μM, ^{3}TPPS* quenching by nitroxide is likely not important.

The TA experiments provide conclusive evidence that neither the starting amine nor the nitroxide photoproduct compete with quenching of the excited photosensitizer. Therefore, it is reasonable to use the reported Φ_Δ value, 0.60,[55,62] in Equation 1.

The Φ_{R2NO} varied linearly with respect to initial TMPD and/or N-TMPCl concentration (Figure 4). The linear response confirms simple first-order kinetics with respect to the amine, indicating that $^1O_2$ quenching by the amine is slow relative to the normal relaxation, τ_Δ^{-1}.

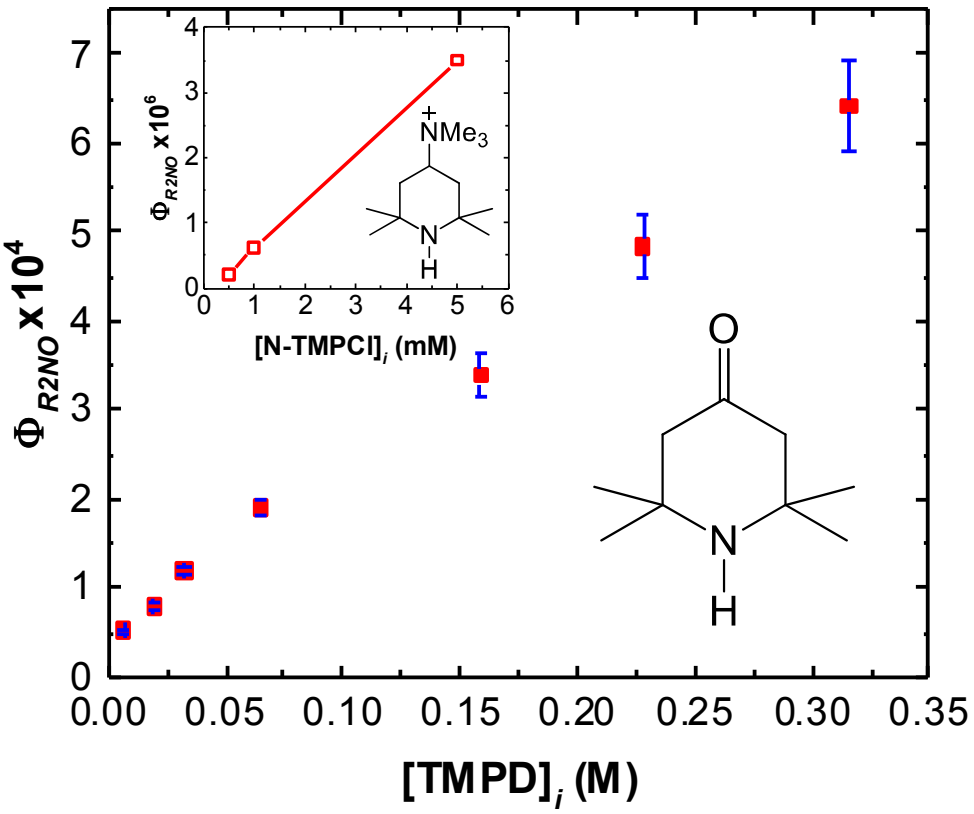

Figure 4. Plot of TEMPOne formation quantum yield versus the initial concentration of TMPD. TMPD•HCl was used at concentrations ranging from 5 to 500 mM in 50 mM aqueous phosphate buffer at *p*H = 8.0. The concentration of TPPS was kept constant at 20 μM. The initial concentration of free base, $[TMPD]_i$, was calculated using the reported pK_a of $TMPDH^+$ (7.6) and the Henderson-Hasselbalch equation. EPR samples were prepared by drawing N_2 de-aerated solutions into 0.5 mm ID glass capillaries and sealed. Insert: similar data plotted for N-TMPCl.

The expression in equation 1 can be simplified based on the observed reaction to, Eq. 2:

$$\Phi_{R2NO} = \Phi_{\Delta}\tau_{\Delta}k_{R2NO}[\mathrm{R_2NH}]_i \quad (2)$$

where the slope of a linear fit to the data in Figure 4 is equal to the quantum yield of singlet oxygen formation times the native lifetime in water times the rate constant for formation nitroxide from free-base amine. Using τ_{Δ} = 3.1 μs[56] and Φ_{Δ} = 0.60,[55] the rate constant for nitroxide formation (k_{R2NO}) from TMPD and N-TMPCl is 1.0 ± 0.1 x 10^4 and 0.4 ± 0.1 x 10^3 $M^{-1}s^{-1}$, respectively. The difference in rate constants between the two substrates reflects a possible difference in driving forces. Future experiments involving deuterium kinetic isotope effects will probe this interesting mechanistic issue further.

Conclusions

This work represents the most accurate measurements of the rate constant for nitroxide formation for these two common substrates to date. An especially critical factor in these determinations is the precise evaluation of the light flux hitting the samples using standard actinometric techniques (see Materials and Methods section). In our analysis of the kinetics (Scheme 2) we have taken into consideration the most probable competing pathways and eliminated their involvement, leading to a simplified and compact mathematical expression for the rate constant k_{R2NO}. The impact of this work is its provision of a quantitative assessment for singlet oxygen production in heterogeneous media such as micelles, vesicles and even live cells, which can be accomplished by running nitroxide forming reactions using isotopically labelled hindered amines with

varying hydrophobicities. In a forthcoming paper, this topological distinction for singlet oxygen production will be clearly demonstrated.[63]

Materials and Methods

Purchased Materials. The photosensitizer 5,10,15,20-tetrakis-(4-sulfunatophenyl)-21,23H-porphyrin·7H_2O (H_6TPPS, TPPS) was purchased from TCI-America (Tokyo) and the effective formula weight (1,060 g/mol) was determined spectrophotometrically using the reported electronic absorption spectrum.[40] All solutions were made using Milli-Q water (18.1 MΩ/cm). Potassium tris(oxalate)ferrate was purchased from Strem Chemical and used as purchased, or was synthesized following reported procedures.[64,65] 2,2,6,6-Tetramethyl-4-piperidone was purchased from Sigma Aldrich and was recrystallized from ethanol prior to use. N-TMPCl was synthesized according to the published procedures.[66,67] Oxygen and ultra-high purity argon tanks were purchased from Air Gas Company.

Electron Paramagnetic Resonance Spectroscopy: EPR samples were prepared by drawing N_2 deaerated solutions into 0.5 mm ID glass capillaries (Sutter Instrument) and sealed. X-Band EPR spectra were recorded on a JOEL JES-FA-100 spectrometer with 100 kHz field modulation. Three EPR spectra were averaged per sample, with each acquired with a 15 min scan rate, 1 sec time constant, 1.0 G modulation width, 2500 amplitude and center field of 3363.5 G.

Nitroxide Calibration: Stock solutions of (4-hydroxy-2,2,6,6-tetramethylpiperidin-1-yl)oxyl (TEMPOL) (0.5 to 10 μM) were made in 50 mM sodium phosphate buffer (pH = 8.0) and bubbled with N_2. The *p*H was adjusted using either conc. phosphoric acid or sodium hydroxide. Baseline distortion for samples with a low concentration of nitroxide was corrected for by

integrating individual hyperfine peak areas, taking great care to integrate over the same regions for each sample.

Photochemical Nitroxide Formation and Actinometry: A typical 15 mL photolysis solution contained 20 μM $TPPS^{4-}$ ($A^{LED} > 4$), 0.5 to 500 mM TMPD-HCl and was buffered to *p*H 8.0 with 50 mM or 60 mM sodium phosphate. The initial concentration of free base, $[TMPD]_i$, was calculated using the reported pK_a of $HTMPD^+$ (7.6) and the Henderson-Hasselbalch equation. Photolysis were performed at ambient temperature in a 35 mL round bottom flask with vigorous stirring to maximize oxygen exchange with pure $O_2(g)$ rapidly flowing over the solution. No measureable difference in the rate of nitroxide formation was observed for solutions bubbled with O_2 or blanketed with fast flowing O_2. All photolyses were performed with 395 nm (FWHM = 10 nm) light from a light emitting diode (LED) that was transferred to the reaction vessel using a liquid light guide, delivering approximately 2 W. Light was attenuated by adjusting the LED power supply (4-100% power). Light flux was measured using the potassium tris(oxalate)ferrate chemical actinometer[68-70] and when supply power = 100%, $q_{n,p} = 2.6 \times 10^{-4}$ einstein/min. The concentration of $TPPS^{4-}$ was varied between 5 and 50 μM, and light absorption was calculated from the integrated product of the photolysis solution absorption spectrum ($1-I/I_o$) and the photon flux normalized spectrum of the light source with respect to wavelength. Samples were photolyzed for 1 min to 50 min and then purged with $N_2(g)$ for 10 min in the dark prior EPR analysis.

Acknowledgements

We thank Dr. M. Kyle Brennaman, Melissa Gish, and Prof. John M. Papanikolas for their invaluable advice and assistance performing the transient absorption experiments. This

research made use of instrumentation funded by the UNC EFRC: Center for Solar Fuels, an Energy Frontier Research Center supported by the U.S. Department of Energy, Office of Science, Office of Basic Energy Sciences, under Award No. DE-SC00010011. MDEF gratefully acknowledges the National Science Foundation for support of this work through grant CHE-1111873.

Electronic Supplementary Information (ESI) available: Included in the supporting information are transient absorption spectra of solutions of TPPS with (Figures S1, S2) or without an oxygen atmosphere (Figures S3, S4), and with (Figures S2, S4) or without (Figures S1, S3) added TMPD. Comparisons between transient decays for different samples probed at a variety of wavelengths are presented (Figures S5-S10) along with lifetime data in each figure caption. Transient decays observed with added TEMPOL are presented indicating quenching of the triplet state by the nitroxide (Figure S11). The results of potentiometric titration of N-TMPCL are shown in Figure S12. Finally, synthesis of the hindered amines and our transient absorption methods are described.

References

1 Y. Lin, R. Trouillon, G. Safina, and A.G. Ewing, *Anal. Chem.,* 2011, 83, 4369.

2 R.R. Allison, H.C. Mota, and C.H. Sibata, *Photodiagn. Photodyn. Ther.,* 2004, **1**, 263.

3 D. Kessel, *Photodiagn. Photodyn. Ther.,* 2004, **1**, 3.

4 A.P. Castano, T.N. Demidova, and M.R. Hamblin, *Photodiagn. Photodyn. Ther.,* 2004, **1,** 279.

5 R.W. Redmond, and I.E. Kochevar, *Photochem. Photobiol.,* 2006, **82,** 1178.

6 P.R. Ogilby, *Chem. Soc. Rev.,* 2010, **39,** 3181.

7 H. Wu, Q. Song, G. Ran, X. Lu, and B. Xu, *Trends Anal. Chem.,* 2011, **30,** 133.

8 J.A. Weil, and J.R. Bolton, *Electron Paramagnetic Resonance: Elementary Theory and Practical Applications*; John Wiley & Sons, Inc.: Hoboken, NJ, 2007; Vol. 2.

9 K. Nakamura, K. Ishiyama, H. Ikai, T. Kanno, Y. Niwano, and M. Kohno, *J. Clin. Biochem. Nutr.,* 2011, **47,** 87.

10 A large number of qualitative studies exist and, while many are supplied here, an exhaustive survey is beyond the scope of this paper.

11 S. Kawanishi, S. Inoue, S. Sano, and H. Aiba, *J. Biol. Chem.,* 1986, **261,** 6090.

12 Y. Iwamoto, H. Yoshika, Y. Yanagihara, and I. Mifuchi, *Chem. Pharm. Bull.,* 1985, **33,** 5529.

13 A. Vogler, and H. Kunkely, *J. Am. Chem. Soc.,* 1981, **103,** 6222.

14 C. Hadjur, A Jeunet, and P Jardon, *J. Photochem. Photobiol. B: Biol*, 1994, **26,** 67.

15 D.R. Cooper, N.M. Dimitrijevic, and J.L. Nadeau, *Nanoscale,* 2010, **2,** 114.

16 K. Ishiyama, K. Nakamura, H. Ikai, T. Kanno, M. Kohno, K. Sasaki, and Y. Niwano, *PLOS One,* 2012, **7,** e37871.

17 J. Martins, L. Almeida, and J. Laranjinha, *Photochem. Photobiol.,* 2004, **80,** 267.

18 S. Kataoka, H. Yasui, M. Hiromura, and H. Sakurai, *Life Sci.,* 2005, **77**, 2814.

19 L.R.C. Barclay, M-C. Basque, and M.R. Vinqvist, *Can. J. Chem.,* 2003, **81,** 457.

20 R. Konaka, E. Kasahara, and W.C. Dunlap, Y. Yamamoto, K.C. Chien, M. Inoue, *Free Rad. Biol. Med.,* 1999, **27,** 294.

21 N. Motohashi, and I. Mori, *J. Chromatography,* 1989, **465,** 417.

22 L. Gao, J. Fei, J. Zhao, H. Li, and J. Li, *ACS Nano,* 2012, **6,** 8030.

23 J.I. Kim, J.H. Lee, D.S. Choi, B.M. Won, M.Y. Jung, and J. Park, *J. Food Sci. C,* 2009, **74,** 362.

24 Y. Lion, M. Delmelle, and A. van der Vorst, *Nature,* 1976, **263,** 442.

25 V.B. Ivanov, V.Y. Shlyapintokh, O.M. Khvpstach, A.B. Shapiro, and E.G. Rozantsev, *J. Photochem.,* 1975, **4,** 313.

26 J. Moan, and E. Wold, *Nature,* 1979, **279,** 450.

27 J. Moan, B. Høvik, and E. Wold, *Photochem. Photobiol.,* 1979, **30,** 623

28 J. Moan, *Acta Chem. Scand. B,* 1980, **34,** 519.

29 Y. Lion, E Gandin, and A. van de Vorst, *Photochem. Photobiol.,* 1980, **31,** 305.

30 K. Reszka, and C.F. Chignell, *Photochem. Photobiol.,* 1983, **38,** 281.

31 A.E. Alegria, C.M. Krishna, R.K. Elespuru, and P. Riesz, *Photochem. Photobiol.,* 1989, **49,** 257.

32 T. Ando, T. Yoshikawa, T. Tanigawa, M. Kohno, N. Yoshida, and M. Kondo, *Life Sci.,* 1997, **61,** 1953.

33 A. Rigo, E. Argese, R. Stevanato, E.F. Orsega, and P. Viglino, *Inorg. Chim. Acta,* 1977, **24,** L71.

34 T. Kondo, and P. Riesz, *Radiat. Res.,* 1991, **127,** 11.

35 S. Dzwigaj, and H. Pezerat, *Free Rad. Res.,* 1995, **23,** 103.

36 N. Miyoshi, V. Mišíc, M. Fukuda, and P. Riesz, *Radiat. Res.,* 1995, **143,** 194.

37 L.-Y. Zang, Z. Zhang, H.P. Misra, *Photochem. Photobiol.,* 1990, **52,** 677.

38 L.P.F. Aggarwal, and I.E. Borissevitch, *Spectrochim. Acta A* 2006, **63,** 227.

39 G.S. Nahor, J. Rabani, F. Grieser, *J. Phys. Chem.*, 1981, **85,** 697.

40 K. Kalyanasundaram, and M. Neumann-Spallart, *J. Phys. Chem.,* 1982, **86,** 5163.

41 I.E. Borrisevitch, T. Tominaga, and C.C. Schmitt, *J. Photochem. Photobiol. A: Chem.,* 1998, **114,** 201.

42 K., Lang, P. Kubát, J. Mosinger, and D.M. Wagnerová, *J. Photochem. Photobiol. A: Chem.,* 1998, **119,** 47.

43 G. Gryn'ova, K.U. Ingold, and M.L. Coote, *J. Am. Chem. Soc.,* 2012, **134,** 12979.

44 H. Ohmori, C. Ueda, K. Yamagata, and M. Masui, *J. Chem. Soc. Prekin Trans. 2,* 1987, 1065.

45 E.S. Kagan, I.Y. Zhukova, V.V. Yanilkin, V.I. Morozov, N.V. Nastapova, V.P. Kashparova, and I.I. Kashparov, *Russ. J. Electrochem.,* 2011, **47,** 1199.

46 N. Sutin, and C. Creutz, *Pure & Appl. Chem.,* 1980, **52,** 2717.

47 D. Mauzerall, *J. Am. Chem. Soc.,* 1960, **82,** 1832.

48 R.A. Marcus, *Annu. Rev. Phys. Chem.,* 1964, **15,** 155.

49 S. Prashanthi, P.H. Kumar, L. Wang, A.K. Perepogu, and P.R. Bangal, *J. Fluoresc.,* 2010, **20,** 571.

50 T. Vidóczy, and P. Baranyai, *Helv. Chim. Acta,* 2001, **84,** 2640.

51 C.G. Martínez, S. Jockusch, M. Ruzzi, E. Sartori, A. Moscatelli, N.J. Turro, and A.L. Buchachenko, *J. Phys. Chem. A,* 2005, **109,** 10216.

52 N.N. Kruk, *J. Appl. Spec.,* 2008, **75,** 174.

53 M. Scholz, R. Dědic, T. Breirenbach, and J. Hála, *Photochem. Photobiol. Sci.,* 2013, **12,** 1873.

54 J.D. Spikes, *Photochem. Photobiol.,* 1992, **55,** 797.

55 R.W. Redmond, and J.N. Gamelin, *Photochem. Photobiol.,* 1999, **70,** 391.

56 A.A. Krasnovsky, *J. Photochem. Photobiol. A: Chem.,* 2008, **196,** 210.

57 R.S. Davidson, and K.R. Trethewey, *J. Chem. Soc. Prekin Trans. 2,* 1977, 169.

58 R.S. Davidson, and K.R. Trethewey, *J. Chem. Soc. Prekin Trans. 2,* 1977, 173.

59 R.S. Davidson, and K.R. Trethewey, *J. Chem. Soc. Prekin Trans. 2,* 1977, 178.

60 E.L. Clennan, L.J. Noe, T. Wen, and E. Szneler, *J. Org. Chem.,* 1989, **54,** 3581.

61 I. Saito, T. Matsuura, and M. Inoue, *J. Am. Chem. Soc.,* 1983, **105,** 3200.

62 C. Schweitzer, and R. Schmidt, *Chem. Rev.,* 2003, **103,** 1685.

63 D.F. Zigler, R.D. Schmidt, L.E. Jarocha, E.C. Ding, I. Kirilyuk, R.B.A. Sykes, S. Miller, V.M. Dipasquale, R. Khatmullin, N.V. Lebedeva, and M.D.E. Forbes, manuscript in preparation.

64 J.I. Olmstead, *J. Chem. Ed.,* 1984, **61,** 1098.

65 R.C. Johnson, *J. Chem. Ed.,* 1970, **47,** 702.

66 N. Jayaraj, M. Porel, M.F. Ottaviani, M.V.S.N. Maddipatla, A. Modelli, J.P. Da Silva, B.R. Bhogala, B. Captain, S. Jockusch, N.J. Turro, and V. Ramamurthy, *Langmuir,* 2009, **25,** 13820.

67 C.L. Kwan, S. Atik, L. and A. Singer *J. Am. Chem. Soc.,* 1978, **100,** 4783.

68 C.G. Hatchard, and C.A. Parker, *Proc. Royal Soc. London A: Math. Phys.,* 1956, **235,** 518.

69 J.N. Demas, W.D. Bowman, E.F. Zalewski, and R.A. Valapoldi, *J. Phys. Chem.,* 1981, **85,** 2766.

70 H.J. Kuhn, S.E. Braslavsky, and R. Schmidt, *Pure & Appl. Chem.* 2004, **76,** 2105.

TOC Graphic